On the Two Types of ENSO

By Tomohiko Tomita and Tetsuzo Yasunari

Institute of Geoscience, University of Tsukuba, Tsukuba, Ibaraki 305, Japan
(Manuscript received 8 November 1991, in revised form 15 February 1993)

Abstract

From 1950 to 1988, 10 ENSO (El Niño-Southern Oscillation) events have occurred. These ENSO events are defined by using the Southern Oscillation index (SOI) and the sea surface temperature (SST) anomaly in the central equatorial Pacific. The ENSO events are classified based on the positive anomaly length of the SST time series: about a year with one northern winter, or two or more years with two northern winters. The shorter one (BO-ENSO) terminates in the following year of the occurrence, and the longer one (LF-ENSO) terminates in the two years after the occurrence. The occurrence and termination of both types have strong phase preference to the seasonal cycle of the mean field, *i.e.*, the seasons between northern winter and northern summer. The occurrence years of each type are as follows; the years of BO-ENSO are 1951, '53, '63, '65, '72, and 1982 (6 cases) and the years of LF-ENSO are 1957, '68, '76, and 1986 (4 cases). Since the occurrence, development, and termination of the both types of ENSO have a seasonal phase preference, composite analysis is used to explain the difference between the two types of ENSO clearly. In the northern winter immediately after the BO-ENSO occurrence, the wind stress anomaly field has a specific clockwise eddy off the east coast of the Philippines. This eddy affects the ocean through Ekman pumping and plays an important role in ENSO termination. The most significant difference between a BO-ENSO and an LF-ENSO is whether this eddy appears or not.

1. Introduction

The phenomenon called ENSO (El Niño-Southern Oscillation) has attracted many researchers as a typical large-scale air-sea interaction since Bjerknes (1966, 1969). This phenomenon has the interannual time scale of 2 to 6 years or so, and has been noted as a major cause of the extreme weather conditions all over the world (*e.g.* Ropelewski and Halpert, 1987; Halpert and Ropelewski, 1992). However, the characteristics of each ENSO seem to be quite different from one to another. It is very important to identify accurately the strength and duration of each ENSO, and the seasonal timing of the occurrence and termination, thereby to understand the mechanism and the effect of ENSO on the global circulation. The long-term forecast also requires physical understanding. One of the most essential purposes of this study is to evaluate and classify with certainty the duration of each ENSO.

The years of ENSO since the 1500's were investigated in detail by Quinn (1978, 1987) from the past records of catastrophic floods in northwestern South America and of cruises in the adjacent sea area, documented in several languages. In addition, Thompson (1984) and Lough and Fritts (1985) determined the past ENSO years from the stratigraphy of the Quelccaya ice cap and tree-ring analysis, respectively. Wang (1992) surveyed the ENSO chronology for the last 600 years from proxy data such as Nile floods, Peruvian floods, Australian draughts, numbers of typhoons landing on China, cooler summers in East Asia, and so on. The ENSO years in this century have already been determined by van Loon and Madden (1981), Rasumusson and Carpenter (1983), and Trenberth (1984), mainly from SST (sea surface temperature) and SOI (the Southern Oscillation index) data.

In terms of the time interval of ENSO, Wyrtki (1975, 1985) pointed out that it was a consequence of the piling up process of warm waters in the western tropical Pacific. Graham and White (1988) and White and Pazan (1989) showed, on the other hand, that the off-equatorial Rossby wave of the ENSO delayed oscillator played an essential role in fixing the period. Enfield and Cid S. (1991) surveyed the relationship between the interval of ENSO and solar activity, by using Quinn's (1987) data, showing that the interval is about 5 years when the solar activity is strong, while it is 3.5 years shorter when the activity is weak.

The past ENSO events were sorted in four levels according to strength by Quinn (1987) and Wang (1992). There is also the classification of ENSO with respect to the interval, such as by Enfield and Cid

S. (1991). Fu *et al.* (1986) classified ENSO events into three types from the zonal gradient pattern of SST in the equatorial Pacific. Yasunari (1985) showed that the major and minor ENSO events could be explained by the superposition of two dominant modes (20–30 and 40–60-month periods), which were detected in the interannual variability of tropical Walker circulation. Barnett (1991) advanced the idea of Yasunari (1985) and classified ENSO events into three categories of strength, according to the relation between amplitude and phase of the two predominant periodic components in interannual variability mentioned above. Lau and Sheu (1988) predicted the two types of the ENSO cycle from the conceptional model: one is the two-year cycle, and the other is the four-year cycle. In the cycle of the conceptional model, the period depends on the positive or negative correlation between the air-sea interaction.

Although ENSO events are classified in various manners as listed above, they have never been classified in terms of the duration. In this study, we propose two types of ENSO, by classifying the duration of the individual events. This classification contributes to an explanation of the relationship between the dominant modes in interannual variability such as that of Rasumusson *et al.* (1990), more concretely. In addition, the difference of the impact on the global weathers, depending upon the type of ENSO, is important, especially regarding the persistence and variability of the global circulation anomalies. The evolution and its seasonality of each type of ENSO are also investigated.

Section 2 of this paper describes the data used. The classifications based on the duration of ENSO and the seasonal evolution of each type are described in Section 3 and Section 4, respectively. The summary and discussion of this study is given in Section 5.

2. Data

In this study, the following three datasets were used.

Sea surface temperature (SST). These data, edited by the United Kingdom Meteorological Office, includes monthly data for the period from January 1854 to February 1989, and is given on 5°×5° lat.-lon. grids from 80°N to 80°S for all longitudes. Missing data were interpolated and extrapolated further as follows. The missing data in the space field were linearly interpolated if the number of neighboring missing data was less than three. The missing data with gaps of more than two grid points were extrapolated by using the regression line and the correlation coefficient between the time series of this grid point and the adjoining grid points. The 1950–1989 data were used for analyses because a number of missing data were noticed before 1950.

The Southern Oscillation index (SOI). The normalized sea-level pressure difference between the maritime continent (Darwin) and the central tropical Pacific (Tahiti) was used. "Monthly Climatic Data for the World", published by the National Oceanic and Atmospheric Administration Environmental Data Service of the USA during the period from January 1950 to June 1989, was the original data source.

The wind stress (WS) data. These data, which are based on ship reports from the National Climatic Data Center, were produced at Florida State University from January 1961 through June 1989 by the month. It covers the area over the tropical Pacific (30°N–30°S, 120°E–70°W) with 2°×2° lat.-lon. grids. These data do not have any missing values, but the quality of some data for 1988 and 1989 is questionable, since they are produced from the "quick-look" product.

3. Classification of ENSO

Figure 1 shows the time-longitude cross section of SST in the equatorial Pacific (5°N–5°S) from January 1950 to February 1989. This figure displays the different features of dominant fluctuation of SST from region to region in the equatorial Pacific. In the eastern Pacific, the annual cycle is evident. The SST rises from northern summer to northern winter and falls from the northern winter to the next northern summer. Hereafter, we adopt the seasons of the northern hemisphere. In the central Pacific, the interannual variability is prominent, so that the warm water in the west spreads eastward and retreats westward. In the western region, SST is usually more than 28.5°C throughout the year.

The oceanographical component of ENSO, namely the El Niño event, is defined as the positive large anomaly in the interannual fluctuation which domains in the central equatorial Pacific (*e.g.* Ramage, 1975; Weare, 1976; Wyrtki, 1975, 1985). The Southern Oscillation is the most representative meteorological component of ENSO. This phenomenon is strongly coupled with the large-scale interannual fluctuation of SST mentioned above (*e.g.* Bjerknes, 1966). Hereafter, we observed the interannual fluctuations of SST in the central equatorial Pacific and SOI as indicators of ENSO.

Looking at this figure more carefully, we note that the warm water expansion from the west, for example around 1987, obstructed the cold SST expansion from the east over two successive years. A similar case is found in the '68 ENSO. On the other hand, in the '82 ENSO, the largest one in this century, the warm SST from the west migrated only for one year, though it spread to the farthest east to reach the Peruvian coast. In this case, following the cold SST, expansion from the east was restored normally. A similar case is noted in the '72 ENSO. Hence, we

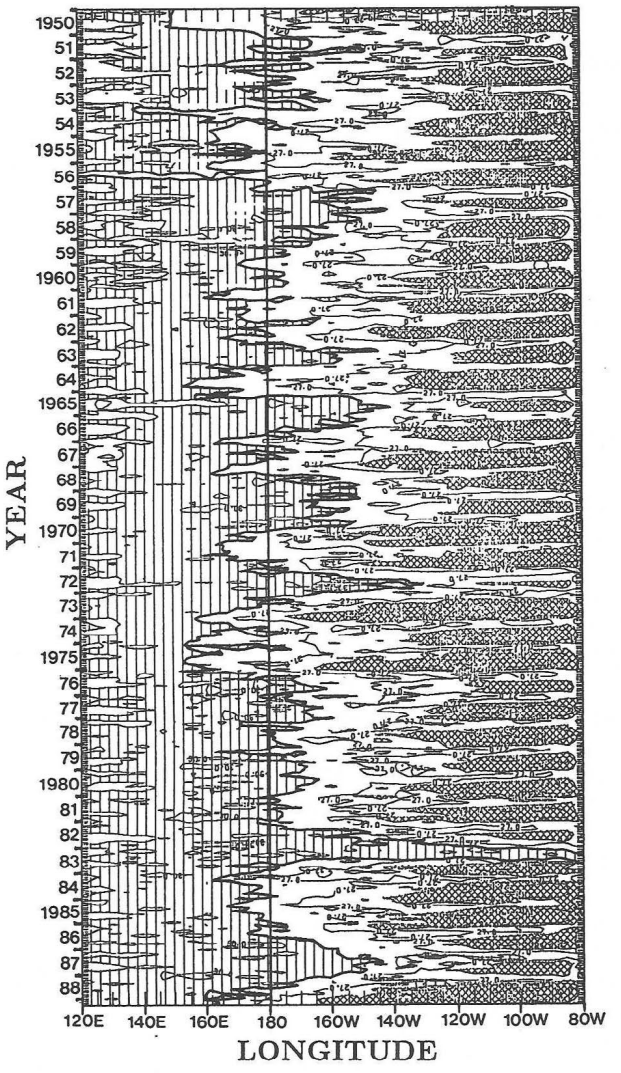

Fig. 1. Time-longitude cross section of SST along the equator from January 1950 to February 1989. The contour interval is 1.5°C and the areas more (less) than 28.5°C (25.5°C) are lightly (darkly) hatched.

classified ENSO events based upon these contrasting features, *i.e.* the duration of events by using the time series of SST in the central equatorial Pacific.

Figure 2 shows the time series of interannual fluctuations of SOI and SST in the central equatorial Pacific (5°N–5°S, 160°E–120°W) from 1950 to 1989. Here SOI was multiplied by a factor of -1 to make it agree in sign with SST. The interannual variability related to ENSO stands out in the central equatorial Pacific, as shown in Fig. 1. In this study, ENSO was defined as the simultaneous swing phase with positive anomalies of each time series exceeding $+1\sigma$ (the standard deviation). The following 10 ENSO events were identified as shown with the year of the occurrence, *i.e.* 1951, '53, '57, '63, '65, '68, '72, '76, '82, and '86. These years were identical to those defined by van Loon and Madden (1981), Rasumusson and Carpenter (1983), Trenberth (1984), Quinn (1987) and others.

By examining the time series of Fig. 2a, we defined the timings of the occurrence and termination of ENSO, when the anomalies turned over from negative to positive and from positive to negative, respectively. The duration of ENSO was, then, deduced as a period between the occurrence and the termination. We also referred to the time series of Fig. 2b as support for the definition. Then we considered the fact that the dispersion of Fig. 2b in the high-period band is larger than that of Fig. 2a, though the correlation coefficient between the two time series is 0.81.

It is noteworthy to state that ENSO events are identifiable as two types, *i.e.*, the longer one, with two maximum peaks, and the shorter one with one maximum peak. The longer events correspond to '57, '68, '76, and '86 ENSOs. The '57 ENSO seems to be the exception, since this event does not have two clear maximum peaks in SST. However, we estimated the event as the longer type because of its long duration. The shorter events are '51, '53, '63, '65, '72, and '82 ENSOs. We did not regard '51 and '53 ENSOs as one event from Fig. 2b, though the separation is subtle in Fig. 2a.

It should be noted that the duration of the negative anomaly before and after each ENSO seems to be closely associated with the duration of the ENSO. For example, the preceding negative phases before the longer ENSO events are longer than those before the shorter ones. Hence we call the longer one an LF-ENSO, which contains the low frequency oscillation, while the shorter one is termed a BO-ENSO, which demonstrates the biennial nature of the swing. These features are more quantitatively discussed in the following.

Table 1 shows the seasons of occurrence and termination, the durations of each type, and the duration of the preceding negative anomalies. The duration of an LF-ENSO is significantly longer than that of a BO-ENSO. An LF-ENSO terminates two years after the occurrence, while a BO-ENSO terminates in the year following the occurrence. The mean durations of an LF-ENSO and the preceding negative phase are 26 and 31 months, while that of a BO-ENSO and its preceding negative phase are 17 and 13 months. The total duration of LF-ENSOs and their preceding negative phases (57 months) is about twice as long as that of BO-ENSOs and their preceding negative phases (30 months). The differences of mean durations between the two types of ENSO are statistically significant with a 99 % confident level or more. The difference between the mean durations of negative phases followed by the two types, however, is not significant.

The seasons of initiation and termination of each

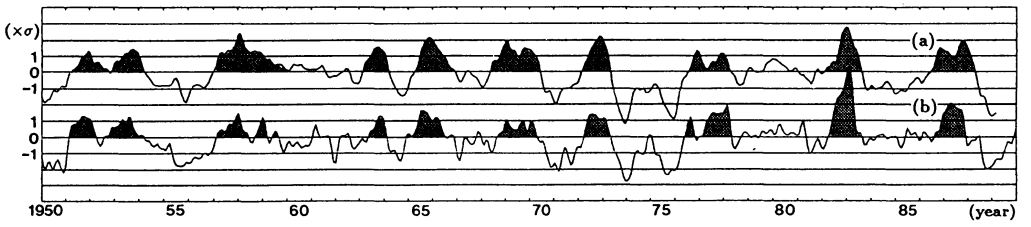

Fig. 2. Time series of normalized anomalies of (a) SST (5°N–5°S,160°E–120°W) and (b) SOI. SOI was multiplied by a factor of −1 to make it agree in sign with SST. The long-term trend was removed, and each line was smoothed by the weighted running mean. These weights were calculated from a normal distribution.

Table 1. The seasonal timing of the initiation and termination of a positive phase and preceding negative phase, and the duration. The unit of duration is one month. Y(0) indicates the year that the ENSO occurred.

BO-ENSO						
	NEGATIVE PHASE			POSITIVE PHASE		
Year	Initiation	Duration	Conversion	Duration	Termination	Total
1951	Spr. 1949	(24)	Spr. 1951	(19)	Aut. 1952	(43)
1953	Aut. 1952	(1)	Win 52–53	(16)	Spr. 1954	(17)
1963	Sum. 1962	(7)	Spr. 1963	(13)	Spr. 1964	(20)
1965	Spr. 1964	(12)	Spr. 1965	(20)	Aut. 1966	(32)
1972	Sum. 1970	(21)	Spr. 1972	(14)	Spr. 1973	(35)
1982	Win. 80–81	(13)	Win 81–82	(18)	Sum. 1983	(31)
Ave.	Win. Y(−1)	(13)	Spr. Y(0)	(17)	Sum. Y(+1)	(30)

LF-ENSO						
	NEGATIVE PHASE			POSITIVE PHASE		
Year	Initiation	Duration	Conversion	Duration	Termination	Total
1957	Spr. 1954	(33)	Win 56–57	(37)	Win. 59–60	(70)
1968	Win. 66–67	(17)	Spr. 1968	(25)	Spr. 1970	(42)
1976	Spr. 1973	(38)	Sum. 1976	(21)	Spr. 1978	(59)
1986	Sum. 1983	(34)	Sum. 1986	(22)	Spr. 1988	(56)
Ave.	Sum. Y(−3)	(31)	Sum. Y(0)	(26)	Spr. Y(+2)	(57)

type are concentrated to winter through summer for almost all events (*cf.* Philander *et al.*, 1984). In particular, strong phase preferences to spring are noted at the initiation of the BO-ENSO and at the termination of LF-ENSO. The seasons of the termination of the LF-ENSO are fixed, though the durations are different by about one year from the durations of the BO-ENSO. The seasons of the initiation of the preceding negative anomalies are also concentrated to winter through summer.

Figure 3 shows composite time series of the two types of ENSO in the time series of Fig. 2. Note the highly coherent fluctuation between SST and SOI. This suggests that the oceanographical and atmospheric components of ENSO evolve coherently on the interannual time scale through the air-sea interaction. It should be emphasized that the BO-ENSO (Fig. 3a) is associated with the biennial-type oscillation from the preceding negative phase to the negative phase after the event. The LF-ENSO, in contrast, seems to occur embedded in the low frequency oscillation of longer time scale from the preceding negative phase, as shown in Fig. 3b. These results give us ample evidence for the two types of ENSO.

4. Evolution of the two types of ENSO

In order to reveal the differences between the spatial and time evolutions of the two types of ENSO, we examine the seasonal (winter and summer) composites of SST and WS anomalies in the tropical Pacific (30°N–30°S, 120°E–80°W). Rasumusson and Carpenter (1982) illustrated similar composite diagrams of unclassified ENSO, which included the 6 cases of '51, '53, '57, '65, '68, and '72 ENSOs. However, since our purpose is to see the differences between the two types of ENSO, it is pointless to compare with the result of Rasumusson and Carpenter (1982), which treats the two types combined together. In this section, we show the composite evolution of the two types of ENSO.

Figure 4 shows the spatial evolution of the BO-ENSO from the winter (WINTER (0) in Fig. 4) immediately before the occurrence to the summer

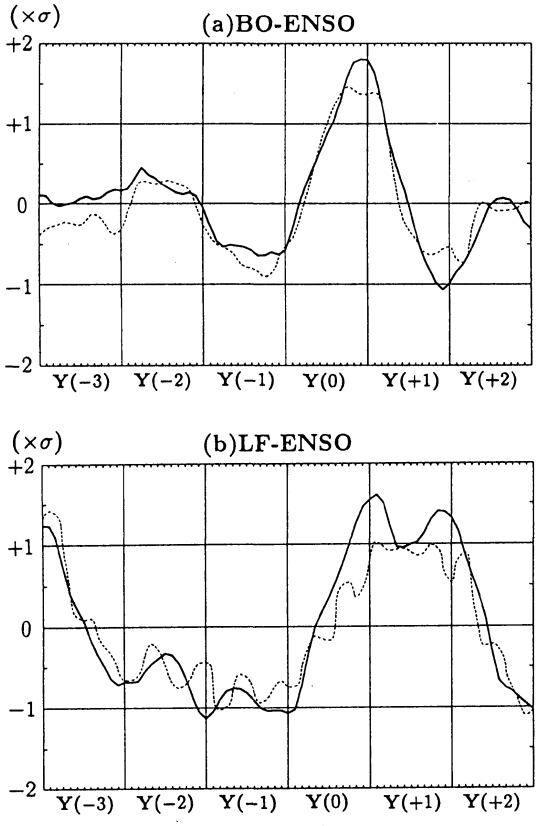

Fig. 3. The composite diagrams of (a) a BO-ENSO and (b) an LF-ENSO using the time series of Fig. 2. Solid (dashed) line indicates the mean SST ($-1 \times$ SOI).

(SUMMER (1) in Fig. 4) in the next year. This period includes the life of the BO-ENSO.

In WINTER (0) (Fig. 4a), large positive anomalies of SST (SSTAs) do not appear. The strong WS anomalies (WSAs), however, have southwesterly components in the central north Pacific (160°E–140°W, 5°N–25°N) and northwesterly components in the eastern tropical Pacific (130°W–80°W, EQ–15°S).

In SUMMER (0) (Fig. 4b), large positive SSTAs appear in the central through eastern equatorial Pacific in the shape of a tongue. To the west of the date line, particularly to the north of Australia, large negative SSTAs are noticeable. The large zonal gradient of SSTAs in the central through western tropical Pacific seem to be coupled with the large WSAs in the western tropical Pacific. Convergence is found in the central equatorial Pacific (180–150°W, 10°N–10°S). This pattern represents the expansion of convective activities relating to the eastward spread of 28°C or warmer water in the west (*cf.* Gadgil *et al.*, 1984; Graham and Barnett, 1987).

In WINTER (1) (Fig. 4c), which corresponds to the mature phase of the BO-ENSO, the large positive SSTAs still persist with a similar pattern to SUMMER (0). Two differences between SUMMER (0) and WINTER (1), however, are found. One is the diminution of the warm region off the west coast of South America and the other is the meridional expansion of the warm region near 160°W. Corresponding to this expansion, the convergence in the central equatorial Pacific enlarged. The north or northeasterly anomalous flows on the north central Pacific (180–160°W, 5°N–25°N) are also strengthened. The other is the remarkable change of anomalous flows from SUMMER (0) to WINTER (1) which occurs in the western tropical Pacific. The large westerly anomalous flows appeared before summer (SUMMER (0)), but turn northeasterly and a large clockwise eddy whose center locates at 140°E, 10°N appears (*cf.* Kutsuwada, 1991). This eddy seems to contribute to the termination of the BO-ENSO through the modulation of the oceanic "Mindanao Dome" (Masumoto and Yamagata, 1991). Positive SSTAs appear off the southeast coast of the Eurasian Continent and north of Australia (*cf.* Hanawa *et al.*, 1989). This pattern suggests that the eddy depends on the heat contrast between the western tropical Pacific and either the Eurasian continent or the east equatorial Indian ocean.

In SUMMER (1) (Fig. 4d), the positive SSTAs in the central through eastern tropical Pacific have obscured and have even reversed their signs. The northeasterly WSAs in the tropical western Pacific do not change, though the clockwise eddy does not appear clearly. In the region of the negative SSTAs, weak divergence appears, especially in the central equatorial Pacific.

Figure 5 shows the spatial evolution of seasonal anomalies of SST and WS for the LF-ENSO. The duration is from the winter (WINTER (0)) immediately before the occurrence to the summer (SUMMER (2)) two years after the occurrence. This duration includes the life of the LF-ENSO.

In WINTER (0) (Fig. 5a), large negative SSTAs appeared in the central through eastern equatorial Pacific (170°W–110°W, 10°N–10°S). A region like this does not appear in WINTER (0) of the BO-ENSO (Fig. 4a), though there is a possibility that the difference depends on the time lag of about one season between the occurrences of the two types of ENSO (see Table 2). To the north and south of this region, the northern or southern WSAs appear, respectively.

In SUMMER (0) (Fig. 5b), the region of the positive SSTAs of ENSO appears around the equator to the east of 160°W, but the region is smaller than that for the BO-ENSO (Fig. 4b). Furthermore, the SSTAs around the maritime continent are slightly positive. The zonal gradient of SSTAs in the western tropical Pacific is smaller than that of Fig. 4b. The westerly WSAs in the western equatorial Pacific seem to be small for this reason. The positive SSTAs

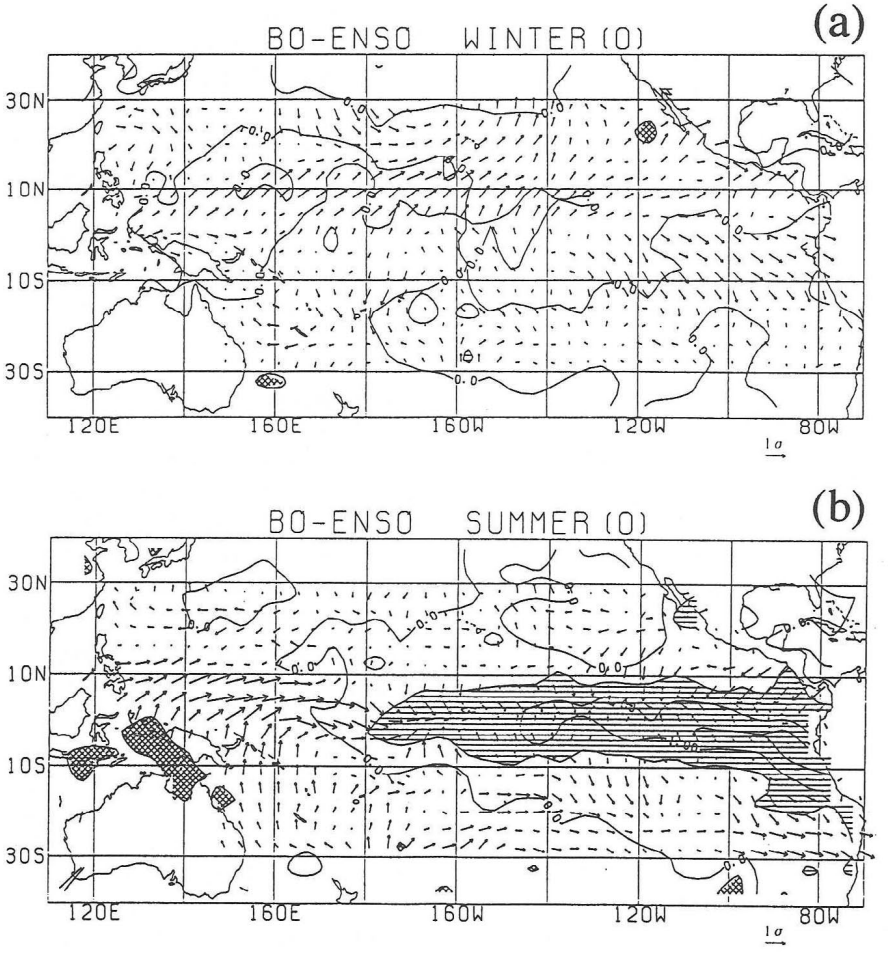

Fig. 4. Evolution of the seasonal composites (winter and summer) of SST and WS anomalies for a BO-ENSO. The contour interval is 0.5°C. Areas over 0.5°C (under −0.5°C) are shaded lightly (darkly). The arrows indicate the direction and the relative size of the normalized WS anomalies. WINTER (0) indicates the winter immediately before the occurrence of a BO-ENSO.

in the region around 145°W–125°W, 20°N–35°N are strikingly different.

In WINTER (1) (Fig. 5c), the region of the positive SSTAs in the central through eastern tropical Pacific expand westward and to higher latitudes. The positive SSTAs around the maritime continent have changed to negative from SUMMER (0), and the westerly WSAs have appeared over the western equatorial Pacific. The large clockwise eddy over the western Pacific shown in WINTER (1) of BO-ENSO (Fig. 4c) has not appeared.

In SUMMER (1) (Fig. 5d), which corresponds with the terminal season of the BO-ENSO, the positive SSTAs are still as large as in WINTER (1) and expand further to the west by about 20° of longitude. However, the region of positive SSTAs off the west coast of South and Central America diminishes. The anomalous flow toward the equator is strengthened over the western through central tropical Pacific, and the westerly WSAs shown in WINTER (1) (Fig. 5c) on the western tropical Pacific disappear.

In WINTER (2) (Fig. 5e), the positive SSTAs spread from the central tropical Pacific to the west coast of North America. The negative SSTAs stay at almost the same location in the north and south at latitude 20 degrees since WINTER (1). The large positive SSTAs in the eastern equatorial Pacific disappear completely. The northwesterly WSAs have appeared again in the western equatorial Pacific, and southeasterly WSAs are shown in the eastern equatorial Pacific. These anomalous flows turned to the region of the positive SSTAs in the central tropical Pacific. The anomalous flows to the equator shown in SUMMER (1) (Fig. 5d) were weakened.

In SUMMER (2) (Fig. 5f), large negative SSTAs are shown in the eastern equatorial Pacific. The slight positive SSTAs appeared widely in the rest of the tropical Pacific. This figure shows the state after the termination of the LF-ENSO. In the central equatorial Pacific, an obvious divergence is found over the negative SSTAs. WSAs on the western tropical Pacific have turned northeasterly from

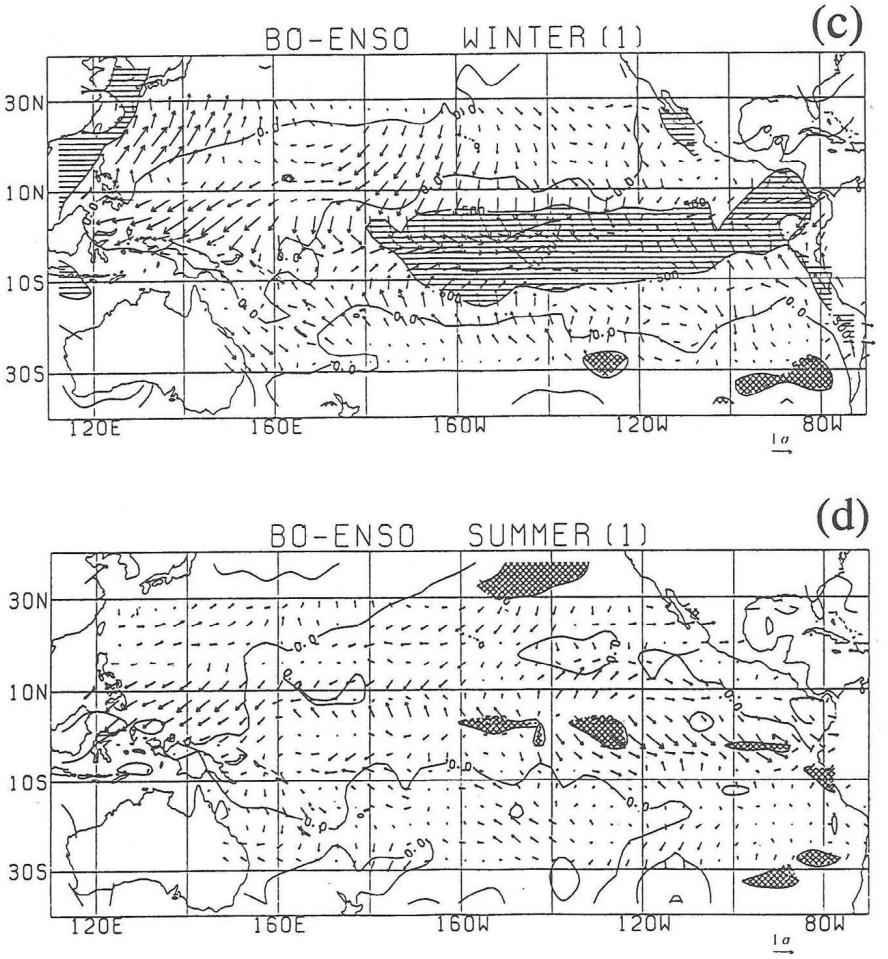

Fig. 4. (Continued)

northwesterly. This change of the direction seems to terminate the LF-ENSO, though the clockwise eddy does not appear in WINTER (2) in the western tropical Pacific.

The fundamental difference between the two types of ENSO is summarized as follows. The clockwise eddy which appears in the western tropical Pacific in WINTER (1) of BO-ENSO is not found in that of the LF-ENSO. This eddy is likely to let the surrounding warm water converge under it through Ekman pumping, and affects greatly the ENSO termination. In the LF-ENSO, with no such eddy, the ENSO state remains unchanged and a warm-water anomaly persists centered in the central equatorial Pacific. This state continues into the next year, but the clockwise eddy, which appeared in WINTER (1) immediately before the BO-ENSO termination, is not as clear in WINTER (2) as in WINTER (1) of the LF-ENSO.

It is also clear that the negative SSTAs spread in the central and the eastern equatorial Pacific are more specific before and after the LF-ENSO than for the BO-ENSO. This fact implies a relation with the long-duration negative anomaly preceding the LF-ENSO (see Fig. 3), but further studies are needed.

5. Summary and discussion

This study classifies ENSO events into two types with respect to their duration, and specifies the differences between the two types of ENSO.

First, we select ENSO events in the time series anomalies of SST in the central equatorial Pacific and SOI, with the criterion whether the positive anomalies of the two time series exceed concurrently the standard deviation or not. With this criterion, 10 ENSO events are selected during the period from 1950 to 1988. These occurrence years are 1951, '53, '57, '63, '65, '68, '72, '76, '82, and '86.

The selected ENSO events are classified into two types according to the duration of the event. We defined the duration by the continuous period of the positive anomalies in the two time series used for the selection of ENSO events. 10 ENSO events after 1950 are classified into two types: one is the biennial oscillatory event, namely the BO-ENSO, and the other is the lower frequency event, that is the LF-ENSO.

The average duration of a BO-ENSO is about 17

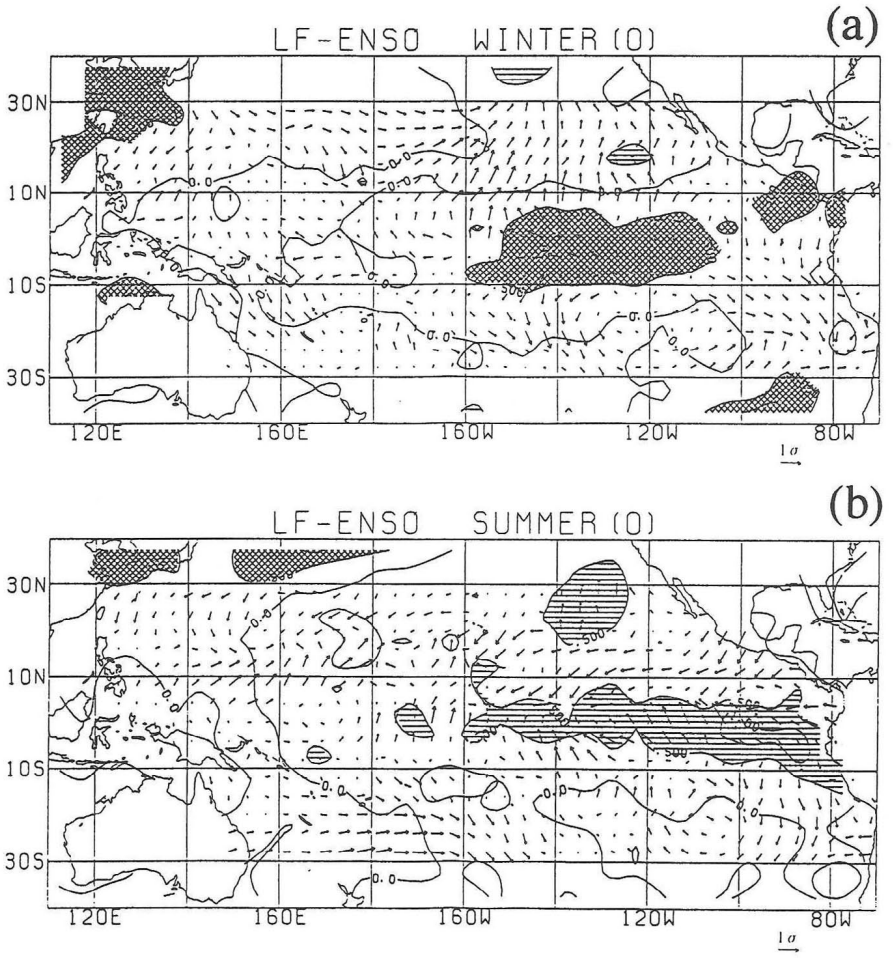

Fig. 5. Evolution of the seasonal composites (winter and summer) of SST and WS anomalies for an LF-ENSO. The contour interval is 0.5°C. Areas over 0.5°C (under −0.5°C) are shaded lightly (darkly). The arrows indicate the direction and the relative size of the normalized WS anomalies. WINTER (0) indicates the winter immediately before the occurrence of an LF-ENSO.

months with one northern winter, and terminates in the year following the occurrence. The years of occurrence are 1951, '53, '63, '65, '72, and '82. The average duration of an LF-ENSO is about 26 months with two northern winters, and terminates in the two years after the occurrence. The occurrence years of the LF-ENSO are 1957, '68, '76, and '86. The number of BO-ENSOs is six and that of LF-ENSOs is four, among the 10 ENSO events. The difference between the average durations of the two types of ENSO is statistically significant with a 99 % confident level or more. The significant difference between the mean durations of negative anomalies preceding the two types of ENSO is also noticed, *i.e.*, about 13 months for the BO-ENSO, and about 31 months for the LF-ENSO. The total mean duration of the negative phase before the LF-ENSO to the following positive phase is about 57 months, which is almost two times longer than that for a BO-ENSO, *i.e.*, about 30 months. Although the duration of an ENSO differs significantly between the two types, both ENSOs tend to initiate and terminate with seasonal phase preference, that is, mostly in the northern winter through northern summer.

By applying a composite analysis, the differences of the time and spatial evolutions of the two types of ENSO are elucidated as follows: Firstly, the positive SST anomalies in the central through eastern equatorial Pacific appear for three successive years in the LF-ENSO, especially in the central equatorial Pacific, while in the BO-ENSO these anomalies disappear by the next northern summer of the occurrence year.

Secondly, in the northern winter of a BO-ENSO, that is, during the mature phase of a BO-ENSO, a clockwise eddy of wind-stress anomalies appears in the western tropical Pacific, and in the following northern summer, easterly anomalies prevail in the western equatorial Pacific (*cf.* Kutsuwada, 1991). No eddy appears, on the other hand, in the corresponding northern winter of an LF-ENSO immediately after the occurrence. The easterly anoma-

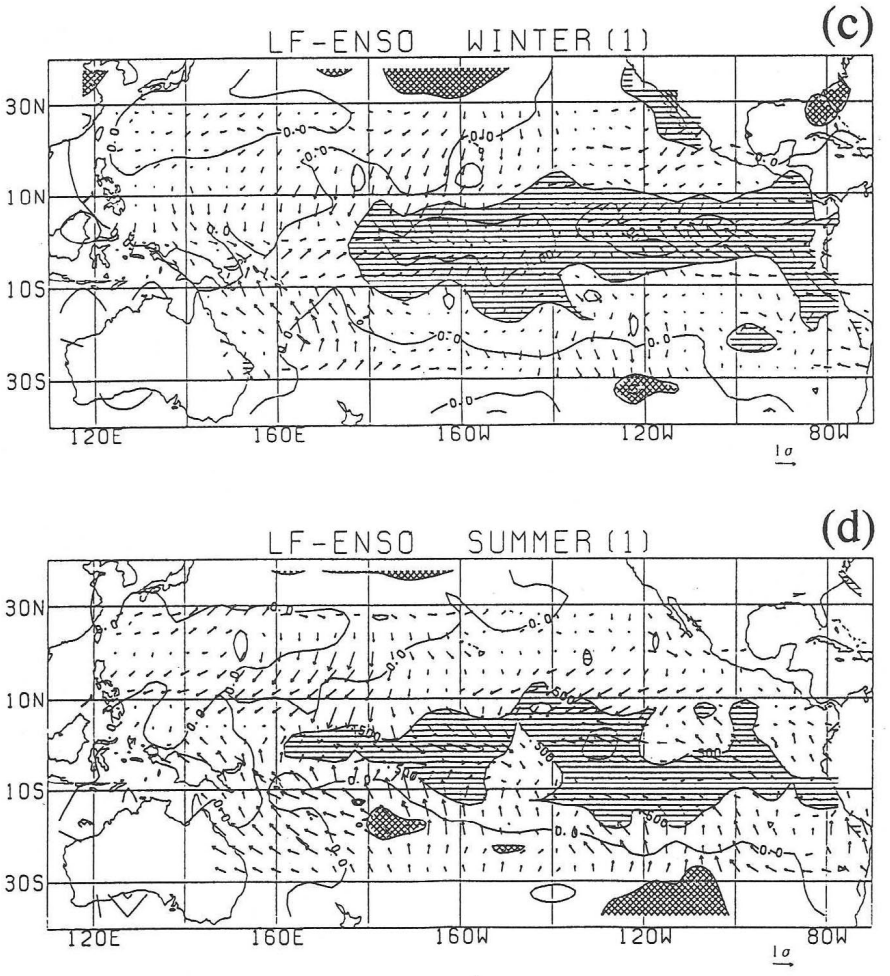

Fig. 5. (Continued)

lies are found in the northern summer two years after the occurrence, although the clockwise eddy does not appear in the northern winter before. The eddy seems to be the most significant phenomenon that characterizes a BO-ENSO. This clockwise eddy of wind-stress anomalies affects the ocean with the modulation of the oceanic "Mindanao Dome" in the western tropical Pacific and plays an important role in an ENSO termination (Masumoto and Yamagata, 1991). In other words, the eddy steadily restores the warm water spread over the western tropical Pacific by Ekman pumping. The observations of wind field suggest that the eddy plays a major role in keeping the biennial oscillation constant, and also suggest that this eddy occurrence is closely related to the anomalous north-south flow off the east coast of the Eurasian Continent in the northern winter. The Asian monsoon system, that is, the air-sea-land system seems to control the termination of an ENSO through this anomalous flow strength, which is strongly affected by the pressure gradient between the Siberian high and the Aleutian low and these center positions. The Asian winter as well as summer monsoon activity is, therefore, suggested to be important for ENSOs (*cf.* Yasunari, 1990, 1992).

Thirdly, before and after an LF-ENSO, the negative SST anomalies in the central through the eastern equatorial Pacific appear more prominently than those before and after a BO-ENSO. The time series analysis clarified that the negative phase before an LF-ENSO is longer than that before a BO-ENSO. Regarding the occurrence of each type of ENSO, the results suggest the importance of the condition before the occurrence, that is, the depth and distribution of the oceanic mixing layer related to the heat content in the western tropical Pacific (*cf.* Masumoto and Yamagata, 1991).

The two types of ENSO classified in this study may be composed into the two types of ENSO suggested by Lau and Sheu (1988) in the conceptional model: one is the two-year cycle, and the other is the four year cycle. The fact that, within the time series of real ENSO factors such as SST or SOI, the two types of ENSO exist together, and that ENSO event can be classified clearly into either type, shows that correlation of the air-sea interaction is in

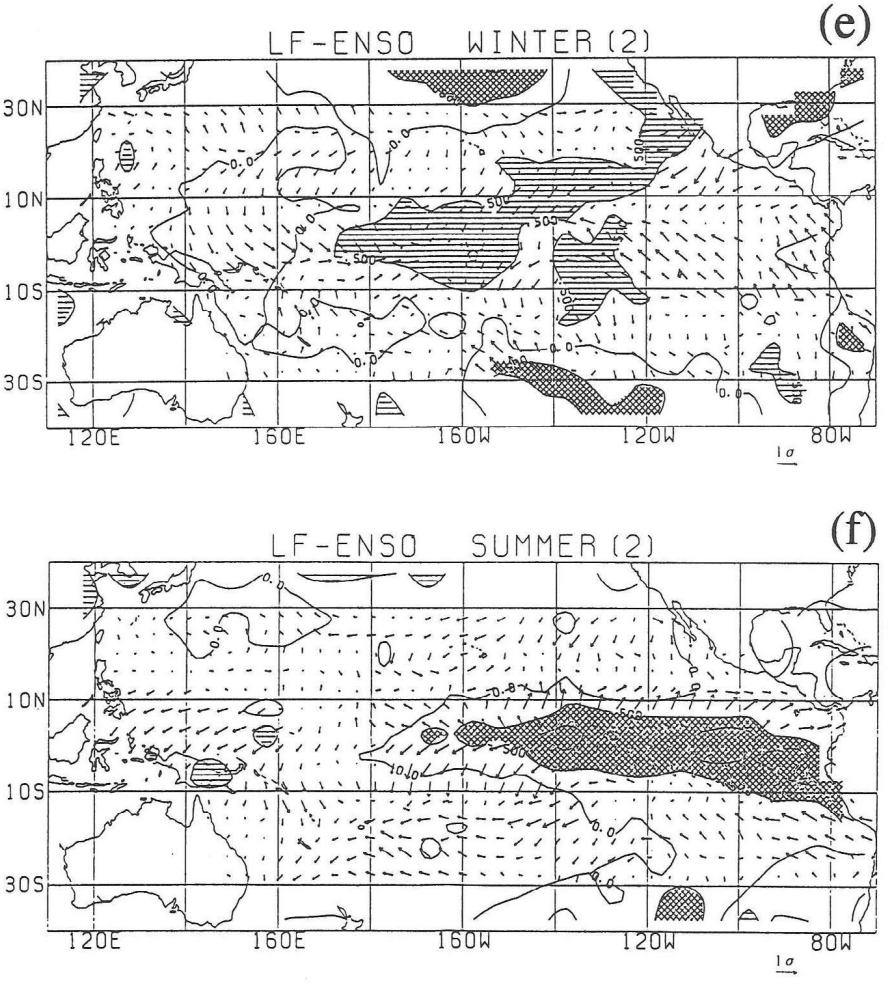

Fig. 5. (Continued)

the ENSO/monsoon system, sometimes positive and sometimes negative. This study strongly suggests that the clockwise eddy in the wind-stress anomaly field over the western tropical Pacific plays the role of a switch of this correlation, and that this switch changes the anomalous condition in the equatorial Pacific, which controls the termination or continuation of an ENSO event.

In the future, these results must be further evaluated quantitatively, with observational or model studies. The scientific results of TOGA (tropical oceans and global atmosphere) are expected to give us further evidence and new ideas about the two types of ENSO.

References

Barnett, T.P., 1991: The interaction of multiple time scales in the tropical climate system. *J. Climate*, **4**, 269–285.

Bjerknes, J., 1966: A possible response of the atomospheric Hadley circulation to the equatorial anomalies of ocean temperature. *Tellus*, **18**, 820–829.

Bjerknes, J., 1969: Atmospheric teleconnections from the equatorial Pacific. *Mon. Wea. Rev.*, **97**, 163–172.

Enfield, D.B. and L. Cid S., 1991: Low-frequency changes in El Niño-Southern Oscillation. *J. Climate*, **4**, 1137–1146.

Fu, C., H.F. Diaz and J.O. Fletcher, 1986: Characteristics of the response of sea surface temperature in the central Pacific associated with warm episodes of the Southern Oscillation. *Mon. Wea. Rev.*, **114**, 1716–1738.

Gadgil, S., P.V. Joseph and N.V. Joshi, 1984: Ocean-atmosphere coupling over monsoon regions. *Nature*, **312**, 141–143.

Graham, N.E. and T.P. Barnett, 1987: Sea surface temperature, surface wind divergence, and convection over tropical oceans. *Science*, **238**, 657–659.

Graham, N.E. and W.B. White, 1988: The El Niño cycle: A natural oscillator of the Pacific ocean-atmosphere system. *Science*, **240**, 1293–1302.

Halpert, M.S. and C.F. Ropelewski, 1992: Surface temperature patterns associated with the Southern Oscillation. *J. Climate*, **5**, 577–593.

Hanawa, K., Y. Yoshikawa and T. Watanabe, 1989: Composite analyses of wintertime wind stress vector fields with respect to SST anomalies in the western

north Pacific and the ENSO events Part II. ENSO composite. *J. Meteor. Soc. Japan*, **67**, 833–845.
Kutsuwada, K., 1991: Quasi-periodic variabilities of wind-stress fields over the Pacific ocean related to ENSO events. *J. Meteor. Soc. Japan*, **69**. 687–700.
Lau, K.-M. and P.J. Sheu, 1988: Annual cycle, quasi-biennial oscillation, and Southern Oscillation in global precipitation. *J. Geophys. Res.*, **93**, 10975–10988.
Lough, J.M. and H.C. Fritts, 1985: The Southern Oscillation and tree reings, 1600–1961. *J. Climate Appl. Meteor.*, **24**, 952–966.
Masumoto, Y. and T. Yamagata, 1991: On the origin of a model ENSO in the western pacific. *J. Meteor. Soc. Japan*, **69**, 197–207.
Masumoto, Y. and T. Yamagata, 1991: The response of the western tropical Pacific to the Asian winter monsoon : The generation of the Mindanao Dome. *J. Phys. Oceanogr.*, **21**, 1386–1398.
Philander, S.G.H., T. Yamagata and R.C. Pacanowski, 1984: Unstable air-sea interactions in the tropics. *J. Atmos. Sci.*, **41**, 604–613.
Quinn, W.H., D.O. Zopf, K.S. Short and R.J.W.K. Yang, 1978: Histrical trends and statistics of the Southern Oscillation, El Niño, and Indonesian droughts. *Fish. Bull.*, **76**, 663–678.
Quinn, W.H. and V.T. Neal, 1987: El Niño occurrences over the past four and a half centuries. *J. Geophys. Res.*, **92**, 14449–14461.
Ramage, C.S., 1975: Preliminary discussion of meteorology of the 1972–73 El Niño. *Bull. Amer. Meteor. Soc.*, **56**, 234–242.
Rasumusson, E.M. and T.H. Carpenter, 1982: Variations in tropical sea surface temperature and surface wind fields associated with the Southern Oscillation/El Niño. *Mon. Wea. Rev.*, **110**, 354–384.
Rasumusson, E.M. and T.H. Carpenter, 1983: The relationship between eastern equatorial Pacific sea surface temperture and rainfall over India and Sri Lanka. *Mon. Wea. Rev.*, **111**, 517–528.
Rasumusson, E.M., X. Wang and C.F. Ropelewski, 1990: The biennial component of ENSO variability. *J. Mar. Sci.*, **1**, 71–96.
Ropelewski, C.F. and M.S. Halpert, 1987: Global and regional scale precipitation associated with El Niño/Southern Oscillation. *Mon. Wea. Rev.*, **115**, 1606–1626.
Thompson, L.G. *et al.*, 1984: El Niño-Southern Oscillation events recorded in the stratigraphy of the tropical Quelccaya ice cap, Peru. *Science*, **226**, 50–53.
Trenberth, K.E., 1984: Signal versus noise in the Southern Oscillation. *Mon. Wea. Rev.*, **112**, 326–332.
van Loon, H. and R.A. Madden, 1981: The Southern Oscillation. Part 1: Global associations with pressure and temperature in northern winter. *Mon. Wea. Rev.*, **109**, 1150–1162.
Wang, S., 1992: Reconstruction of El Niño event chronology for the last 600 year period. *Acta Meteorologica Sinica*, **6**, 47–57.
Weare, B.C., A.R. Navato and R.E. Newell, 1976 : Empirical orthogonal analysis of Pacific sea surface temperatures. *J. Phys. Oceanogr.*, **6**, 671–678.
White, B.W. Y. He and S.E. Pazan, 1989: Off-equatorial westward propagating Rosbby waves in the tropical pacific during the 1982–83 and 1986–87 ENSO events. *J. Phys. Oceanogr.*, **19**, 1397–1406.
Wyrtki, K., 1975: El Niño—The dynamic response of the equatorial Pacific ocean to atmospheric forcing. *J. Phys. Oceanogr.*, **5**, 572–584.
Wyrtki, K., 1985: Water displacements in the Pacific and the genesis of El Niño cycles. *J. Geophys. Res.*, **90**, 7129–7132.
Yasunari, T., 1985: Zonally propagating modes of the grobal east-west circullation associated with the Southern Osillation. J. Meteor. Soc. Japan, 63, 1013-1029.
Yasunari, T.,1990: Impact of Indian monsoon on the coupled atmosphere/ocean system in the tropical Pacific. *Meteor. & Atmos. Phys.*, **44**, 29–41.
Yasunari, T., 1992: Role of the Asian Monsoon on the Interannual Variability of the Global Climate System. *J. Meteor. Soc. Japan*, **70**, 177–189.

2つのタイプのENSOについて

冨田智彦・安成哲三
(筑波大学地球科学系)

1950年以降の10例のENSO(エルニーニョ/南方振動) について、期間に着目した分類を試みた。ENSOは、期間に着目すると、発生年の翌年に終息するタイプ (BO-ENSO) とそのさらに翌年まで継続するタイプ (LF-ENSO) の2つのタイプに分類できる。そしてどちらのタイプのENSOについてもその発生、終息の時期は、北半球の冬から夏にかけての季節に集中している。発生年で両者を示すとBO-ENSOは、1951, '53, '63, '65, '72, '82年の6例、LF-ENSOは、1957, '68, '76, '86年の4例であった。次に両者の発生、発達、終息には明瞭な季節固定があることより、合成解析を行い両者の違いを明らかにした。風応力の偏差

場においてBO-ENSOの発生直後の冬季、フィリピン東岸沖に時計回りの明瞭な渦が見られる。対応するLF-ENSOの発生直後の冬季には、この様な渦は出現していない。この渦は、EkmanPumpingを介して海洋に作用しENSOの終息に大きく寄与していると考えられる。BO-ENSOとLF-ENSOを分ける要因の一つとしてこの渦の出現の有無をあげる。